

Measured Ionospheric Delay Corrections for Code-based GPS Time Transfer

Victor Zhang and Zhiqi Li

Abstract: In Global Positioning System (GPS) time transfer measurements, all of the delays in receiving GPS timing signals, including the ionospheric delay in the signal path and the internal delay of a GPS receiver (receiver delay), must either be corrected for or included in the uncertainty analysis. For code-based GPS time transfer with single frequency receivers, the ionospheric delay can be corrected using the Klobuchar model, or using the IGS ionospheric maps. The modeled ionospheric delay correction is most effective during the nighttime hours. The IGS ionospheric map corrections have much smaller uncertainties than corrections from the Klobuchar model, especially during the daytime hours, but the effects of ionosphere variations are still noticeable in the received GPS signals due to the resolution of the map. With the use of dual-frequency multi-channel GPS receivers, the ionospheric delay can be obtained from the receiver's dual-frequency measurements. The measured ionospheric delay correction removes nearly all of the ionospheric delays from the GPS time measurements. However, the receiver delay for the measurements on both the L1 and L2 frequencies are used in computing the ionospheric delay, and if the receiver delay is not calibrated or if the delay has changed, the error in receiver delay can propagate to the measured ionospheric delay corrections, and add uncertainty to the time transfer results. Thus, to achieve the lowest possible time transfer uncertainty, it is important to locally monitor receiver delay changes and to periodically calibrate the receiver delay.

1. Introduction

The Global Positioning System (GPS) satellites transmit radio frequency (RF) signals for position, navigation, and timing applications. Single frequency devices receive the L1 band carrier frequency (1575.42 MHz) and dual-frequency devices receive both the L1 and L2 (1227.60 MHz) carrier frequencies. The GPS signals contain accurate time and frequency information. For example, both GPS system time (GPST) and Coordinated Universal Time (UTC), as maintained by the U. S. Naval Observatory (USNO), are embedded in the GPS navigation messages. The GPST is derived from the composite clock, which consists of the atomic clocks on board the satellites and at ground control stations. The orbital parameters of the GPS satellites are also contained in the navigation messages.

In GPS time transfer applications, the GPS receivers are typically installed in stationary positions with fixed coordinates. The receiver clock, or latch point of the measurements, is synchronized on the timing reference clock. The pseudo-ranges therefore give a measure

of the differences between the reference clock and the GPST. Even if the pseudo-ranges are generally expressed in unit of distances, we will here consider them as the measurements of the satellite to receiver travel time, after division by the speed of light; hence they are expressed in seconds. With the knowledge of the satellite's position and the receiving antenna's coordinates, the pseudo-range measurements can be corrected by the propagation delay between the satellite and receiver. This range delay measurement result is used to extract the GPS timing information. In addition to the range delay, the ionosphere and the receiving equipment also introduce delays in the received GPS time. To reduce the timing uncertainty to a minimum, all of these delays must be compensated for or removed from the pseudo-range measurements.

The variations in the ionospheric delay are mainly due to solar radiation and activity. The ionosphere adds group delay to the propagation of GPS pseudo random noise (PRN) codes and advances the phase of GPS carrier frequencies. It can also bend the signal path to make the

path a little longer than a straight path, and can rotate the polarization of the PRN code signal.

The Klobuchar model utilizes eight broadcast coefficients obtained from the navigation message as its inputs [1, 2], and has been used for ionospheric delay corrections since the beginning of GPS. This approach removes about 50 % of the ionospheric errors

Authors

Victor Zhang¹
victor.zhang@nist.gov

Zhiqi Li^{1,2}
zhiqi.li@nist.gov

¹Time and Frequency Division
National Institute of Standards
and Technology
325 Broadway
Boulder, Colorado, 80305

²School of Electro-Mechanical
Engineering, Xidian University
No.2 Taibai Road,
Xi'an, Shannxi, China

```

GGTTS GPS DATA FORMAT VERSION = 01
REV DATE = 2014-6-30
RCVR = NovAtel           L1L2W           SWU04029169   TSNCg2-3.02-X2T           2.200S49           2.100   2012/Dec/12   17:14:15
CH = 11
IMS = IGS estimates
LAB = NIST
X = -1288398.360 m
Y = -4721697.040 m
Z = 4078625.500 m
FRAME = WGS84
COMMENTS = Latitude = 39.99506714 (deg) WGS84
INT DLY = -44.7 ns (GPS L1), -44.7 ns (GPS L2)
CAB DLY = 275.5 ns (GPS)
REF DLY = 114.5 ns
REF = UTC (NIST)
CKSUM = 92

PRN CL  MJD  STTIME  TRKL  ELV  AZTH  REFSV      SRSV  REFGPS  SRGPS  DSG  IOE  MDTR  SMDT  MDIO  SMDI  MSIO  SMSI  ISG  CK
      hhmsss  s .ldg .ldg  .lns      .lps/s  .lns      .lps/s  .lns      .lps/s  .lns      .lps/s  .lps/s  .lps/s  .lps/s  .lps/s  .lps/s  .lps/s
1  FF 56658 000200  780 380 2689  -974108    -14    -49     +12    3 056  127  +5  229  -19  150 9999 999 E0
11 FF 56658 000200  780 213 2423  +4516360   +46   -129    +13    5 082  215  +42 335  -3  229 9999 999 F2
14 FF 56658 000200  780 343  670  -2060919   +13    -82     +2    3 082  138  +19 214  -11  126 9999 999 D6
20 FF 56658 000200  780 291 3101  -1492176   +21   -89     +53    4 021  160  -34 267  -73  162 9999 999 00
22 FF 56658 000200  780 154 1335  -2040967   -50   -72     -26    4 041  291  +119 330  +6  230 9999 999 FD
23 FF 56658 000200  780  94 2729  -166340   +129  -237    +96    4 081  467  -231 451 -115 283 9999 999 3B
25 FF 56658 000200  780 236  589  -62236     -17  -107    +8     4 068  194  +11 254  -31  142 9999 999 D9
31 FF 56658 000200  780 805  862  -3318367   +17   -12     +22    2 052  79   +1  143  -18  93 9999 999 CD
 1  FF 56658 001800  780 355 2600  -974139   -36   -54    -10    1 056  135  +11 229  +6  152 9999 999 D0
11 FF 56658 001800  780 169 2366  +4516379   +6   -142   -27    1 082  266  +69 356  +30 251 9999 999 1D
14 FF 56658 001800  780 291  727  -2060918   -2   -93    -14    1 082  160  +27 217  +6  128 9999 999 D5
20 FF 56658 001800  780 357 3092  -1492173   +3   -55    +35    1 021  134  -22 220  +39  138 9999 999 EB
22 FF 56658 001800  780  92 1365  -2041047  -112  -130   -89    3 041  475  +322 355  +33 280 9999 999 27
23 FF 56658 001800  780 141 2778  -166271   +54  -200   +21    3 081  317  -108 376  -65 245 9999 999 1F
25 FF 56658 001800  780 217  518  -62266     -33  -113   -8     0 068  211  +24 243  -6  132 9999 999 BD
31 FF 56658 001800  780 751  578  -3318369   -10   -9     -6     1 052  81   +3  136  -5  87 9999 999 A7

```

Figure 1. CGGTTS format data generated by the NIST primary timing receiver. The items highlighted in blue are discussed in the paper.

under normal solar activity and is still used by most single frequency GPS time transfer applications.

Because the ionospheric effect on GPS signals is dispersive (frequency dependent), far more accurate ionospheric delay corrections can be obtained by dual-frequency pseudo-range measurements. With the availability of dual-frequency GPS receivers and the development of codeless and semi-codeless techniques in the late 1990s, the International GNSS (Global Navigation Satellite System) Service (IGS) now produces global maps of total electron content (TEC) in the IONosphere map EXchange (IONEX) format [3]. This map is based on measurements obtained from dual-frequency receivers in the IGS worldwide tracking network. Using the IONEX map, we can compute the ionospheric delay for receiving PRN codes from a specific GPS satellite at a explicit location at a given time. This approach does a better job than the Klobuchar model, in all types of solar activity conditions, of reducing the uncertainty of the ionospheric delay correction. Due to the resolution of the IONEX maps (in both epoch time and grid increments), some errors remain in the results. In addition, the IONEX final product is not available in real-time, it has several days of latency. Newer global ionosphere maps, such as the Global Ionosphere Maps (GIM) [4], and regional maps [5, 6, 7] are also available for the ionospheric delay correction. Unfortunately, these newer maps have yet to be used for time and frequency applications.

In recent years, most of the international timing laboratories have obtained dual-frequency, multi-channel receivers. Instead of using the modeled ionospheric delay corrections or the IONEX map, these receivers can obtain ionospheric delay locally from the linear combination of the dual-frequency measurements. This is the most accurate approach in eliminating the ionospheric delay which is also available in near real-time.

The GPS PRN codes are also delayed by the receiving equipment. In this study, we treat the receiver delay as a sum of the receiver’s internal

delays, the antenna delays, and the antenna cable delays. The receiver delay may change as a function of time, local environment, and the quality of the components.

In the code-based remote clock comparison applications, GPS timing receivers record the difference of a reference clock and GPST ($REF - GPS$) from the pseudo-range measurements. The differences are generated in the format recommended by the Consultative Committee for Time and Frequency (CCTF) Group on GNSS Time Transfer Standards (CGGTTS) [8, 9]. An example of data in this format is presented in Fig. 1. Version 1 of the CGGTTS format is only for GPS measurements, but version 2 expands the measurements to include the GLObal NAVigation Satellite System (GLONASS) developed and maintained by the Russian Federation. Data in the CGGTTS format are mostly used by national metrology institutes (NMIs) and other high level timing laboratories that compare their clocks by utilizing either the common-view [10] or the all-in-view [11, 12] time transfer techniques.

The CGGTTS data measurements are stored in 16-minute segments. The difference of $REF - GPS$ obtained from the measurements to each GPS satellite in a 16-minute segment is shown in the REFGPS column. The REFGPS measurements have already been corrected for all associated delays. The modeled ionospheric delay based on the Klobuchar model is shown in the MDIO column. The measured ionospheric delay is shown in the MSIO column. The reference signal delay (REF DLY), the antenna cable delay (CAB DLY) and the receiver internal delays for the L1 and L2 frequencies ($INT DLY_{L1}$ and $INT DLY_{L2}$) are reported in the CGGTTS file header. When measured ionospheric delay corrections are being utilized, this is indicated by the parameter of the Ionospheric Measurement System (IMS), also in the file header. For REFGPS measurements that have been corrected with the MDIO (REFGPS_{MDIO}), we first have to add the MDIO back and then

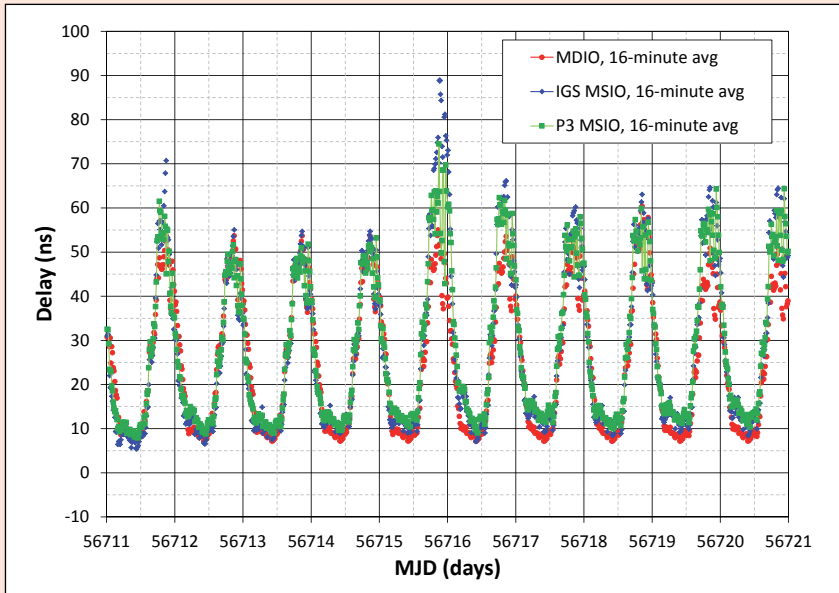


Figure 2. Ionospheric delay corrections for the UTC(NIST) – GPST measurements from February 23 to March 4, 2014.

subtract the MSIO from the REFGPS values in order to implement the MSIO corrections, i.e. $REFGPS_{MSIO} = REFGPS_{MDIO} + MDIO - MSIO$.

In recent years, software has become available that generates the version 2 CGGTTS format data from the Receiver INdependent EXchange (RINEX) formatted data [13]. The RINEX data are produced by dual-frequency, multi-channel global navigation satellite system (GNSS) receivers. The REFGPS measurements obtained from this approach are the “ionosphere-free” difference between a reference clock and GPST. The ionospheric delay correction for the ionosphere-free (P3) difference is the linear combination of the pseudo-range measurements on the L1 and L2 frequencies. To maintain backward compatibility with existing common-view and all-in-view software, both the MDIO and MSIO columns contain the same value of measured ionospheric delay on the L1 frequency using the P3 method.

In Section 2, we examine the error in ionospheric delay correction using the Klobuchar model (MDIO), the MSIO of the IGS IONEX maps (IGS MSIO), and the MSIO of P3 method (P3 MSIO) techniques. We then study the error in P3 MSIO correction introduced by the receiver delay change in Section 3. A summary is presented in Section 4.

2. Error in Ionospheric Delay Correction

Ionospheric delay is dependent on the GPS signal’s propagation path. This is why the values of MDIO and MSIO at the same epoch are different for each GPS satellite as seen in Fig. 1. In general, the ionospheric delay is smaller for a satellite at high elevation because the GPS signal travels a shorter path through the ionosphere. The ionospheric delay in the GPS pseudo-range measurements also varies at different times of the day (daytime or nighttime), at different locations (the latitude of the receiver relative to the equator), and in different seasons. Significant deviations from the normal ionospheric delay occur during solar flares and geomagnetic storms caused by an interaction between solar activity, the ionosphere, and the Earth’s magnetic field.

At the National Institute of Standards and Technology (NIST) in Boulder, Colorado, GPST is continuously compared to the NIST realization of UTC, known as UTC(NIST). Figure 2 shows the ionospheric delay corrections for the UTC(NIST) – GPST obtained from the Klobuchar model (MDIO), the IGS maps (IGS MSIO), and dual frequency measurements (P3 MSIO) for the Modified Julian Dates (MJDs) from 56711 to 56720 (February 23 to March 4, 2014). The ionospheric delay corrections are those reported in the MDIO and MSIO columns in the CGGTTS format data files. Each data point in the plot is an average of the MDIO or MSIO values for

measurements from different GPS satellites in the same 16-minute segment. The averaged ionospheric delay for the pseudo-range measurements ranged from about 5 ns (nighttime) to about 60 ns (daytime) in February 2014. The ionospheric delay reached 90 ns during a geomagnetic event on MJD 56715 (February 27, 2014) [14].

Figure 3 shows the UTC(NIST) – GPST measurements with the MDIO, IGS MSIO, and P3 MSIO corrections from MJD 56711 to MJD 56720 (February 23 to March 4, 2014). The differences are obtained from the pseudo-range measurements as reported in the REFGPS column of the CGGTTS format data files. Each point in a difference plot is an all-in-view difference of $REF - GPS$, the non-weighted average of the measurements to all of the GPS satellites in view during a 16-minute segment. The measurements are offset to show the effectiveness of each correction. We see that UTC(NIST) – GPST with the MDIO correction (shown in red) still contains a large amount of residuals of the ionospheric delay, as indicated by the diurnal structure. The peak on MJD 56715 (February 27, 2014) was due to a geomagnetic event, that started in late morning and lasted until early evening in Colorado (note that this peak was during the daylight hours in Colorado and that UTC was seven hours ahead of local time). The IGS MSIO correction (shown in blue) removes most of the diurnal structure and the impact of the geomagnetic event. However, the difference contains 2 to 10 ns of short term variations most likely due to the resolution uncertainty of the IONEX map. The P3 MSIO correction (shown in green) produces the best result of removing the ionospheric delay from the UTC(NIST) – GPST difference. On MJDs 56712 and 56713 (February 24 and 25, 2014), the ionosphere was relatively quiet and the peak-to-peak variation in the difference is about 2 ns. The difference still shows a diurnal structure with a peak-to-peak variation of up to 6 ns on other days, due to factors other than ionospheric delays, including delay variations of the receiving equipment or multipath signal reflections.

3. Error in the P3 Measured Ionospheric Delay Correction

The ionosphere-free measurements for time transfer applications are computed from the linear combination of

$$\begin{aligned}
 P_3 &= \frac{f_1^2}{f_1^2 - f_2^2} \cdot (P_1 - INT DLY_{L1}) \\
 &- \frac{f_2^2}{f_1^2 - f_2^2} \cdot (P_2 - INT DLY_{L2}) \\
 &= 2.54 \cdot (P_1 - INT DLY_{L1}) - 1.54 \cdot \\
 &(P_2 - INT DLY_{L2}), \quad (1)
 \end{aligned}$$

where $f_1 = 1575.42$ MHz, $f_2 = 1227.6$ MHz are the GPS L1, L2 frequencies respectively; P_1 , P_2 are the pseudo-range measurements on the f_1 and f_2 frequencies; and the $INT DLY_{L1}$, $INT DLY_{L2}$ are the receiver internal delays for the P_1 and P_2 measurements. In the P3 CGGTTS format data files, the modeled and measured ionospheric delays for the measurements on the L1 frequency are obtained from the difference of $(P_1 - INT DLY_{L1}) - P_3$. In addition to the P3 CGGTTS data, some dual-frequency receivers also use this measured ionospheric delay from the P3 method as the MSIO in the single-frequency CGGTTS data files. Because the ionospheric delay obtained from the P3 method includes the receiver internal delays, any variation and error in $INT DLY_{L1}$ and $INT DLY_{L2}$ will affect the time transfer results. The error in $REF - GPS$ due to the errors in ionospheric delay correction is given by

$$\begin{aligned}
 \Delta(REF - GPS)_{P3} &= -[2.54 \cdot \Delta(INT DLY_{L1}) \\
 &- 1.54 \cdot \Delta(INT DLY_{L2})]. \quad (2)
 \end{aligned}$$

In Eq. (2), the term on the right-hand side of the equation is the error in the ionospheric delay correction caused by receiver delay error. The minus sign is due to the fact that delays are subtracted from the pseudo-range measurements.

Eq. (3) and Eq. (4) show the relationship between the ionospheric delay corrected $REF - GPS$ and the receiver delay. For GPS time transfer using MDIO or IGS MSIO corrections,

$$\begin{aligned}
 (REF - GPS)_{\text{iono corrected}} &= (P_1 - INT DLY_{L1}) \\
 &- \text{other delays.} \quad (3)
 \end{aligned}$$

For GPS time transfer that applies the P3 MSIO correction,

$$\begin{aligned}
 (REF - GPS)_{\text{iono-free}} &= 2.54 \cdot (P_1 - INT DLY_{L1}) \\
 &- 1.54 \cdot (P_2 - INT DLY_{L2}) - \text{other delays} \\
 &= (P_1 - INT DLY_{L1}) - \text{other delays} + 1.54 \cdot \\
 &[(P_1 - INT DLY_{L1}) - (P_2 - INT DLY_{L2})], \quad (4)
 \end{aligned}$$

where “other delays” includes the satellite-receiver travel time, the tropospheric delay, the satellite clock error, and multipath noise.

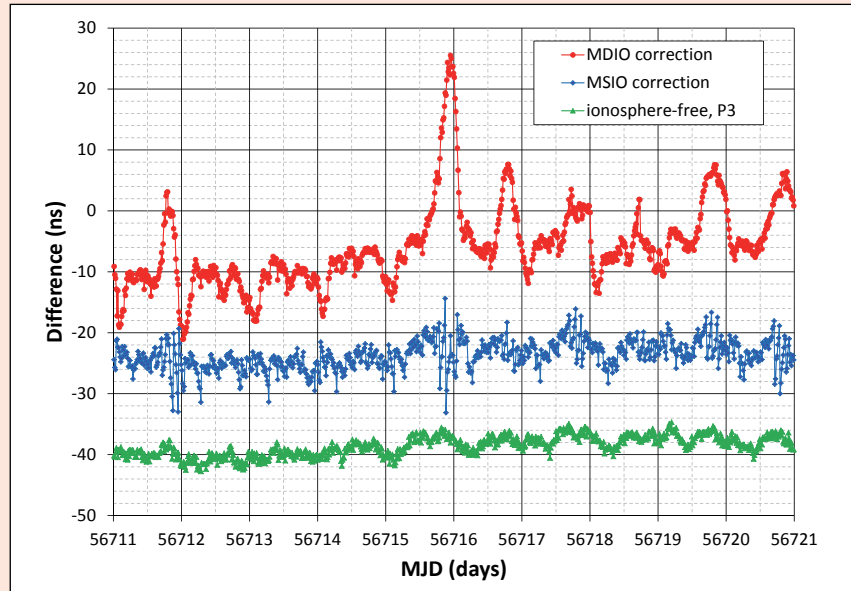


Figure 3. Differences of UTC(NIST) - GPST from February 23 to March 4, 2014 with different ionospheric delay corrections. Each point in a difference plot is an all-in-view difference of $REF - GPS$, the non-weighted average of the measurements to all of the GPS satellites in view during a 16-minute segment. The differences are offset for the purpose of better illustrating the variation in different ionospheric delay correction techniques.

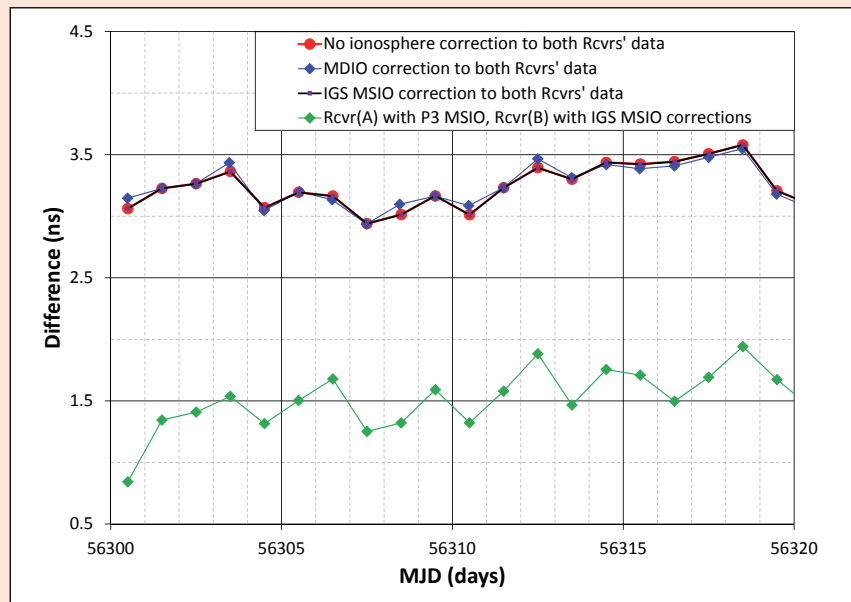


Figure 4. Daily averaged common-clock, common-view differences of two colocated receivers, Rcvr (A) and Rcvr (B). The differences are computed with different ionospheric delay corrections. The MDIO corrections generated by one of the receivers contained many outliers. The $REF - GPS$ data corrected by the MDIO outliers are not used in the daily averaged common-clock, common-view difference. The non-zero differences indicate error in the receiver delay correction.

If the delays on L1 and L2 frequencies are changed, the last term in Eq. (4) adds error to the time transfer results. However, the error in

time transfer due to the receiver delay change as shown by Eq. (2) can also be reduced if both delays change in the same direction, or

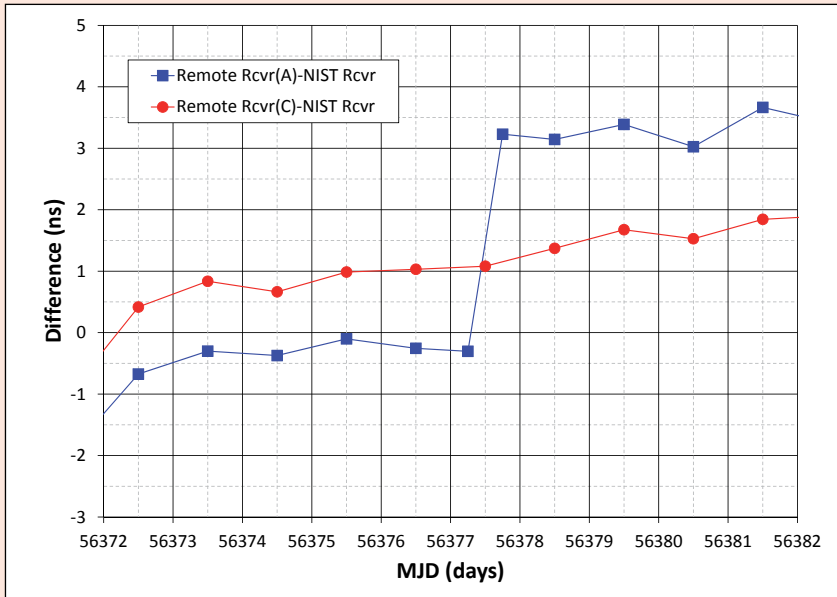


Figure 5. Daily averaged common-view differences of UTC(NIST) – remote clock with P3 MSIO corrections. The measurements at the remote clock location were made by Rcvr (A) and Rcvr (C). The measurements at NIST were made by the NIST primary timing receiver. The Rcvr (A) receiver delay change caused the time step in the common-view difference. The two points on MJD 56377 are the averaged differences before and after the time step.

can even be canceled if $2.54 \cdot \Delta INT DLY_{L1} = 1.54 \cdot \Delta INT DLY_{L2}$.

In Fig. 4, we show the effect of error in the receiver delay on the ionospheric delay correction obtained from the P3 method. Rcvr (A) and Rcvr (B) are two receivers operated in the same location. Rcvr (A) is a dual-frequency, multichannel receiver, and Rcvr (B) is a single frequency, multichannel receiver. The two receiver’s antennas are only 8.7 m apart, so the GPS signals received by the two receivers should have almost the same ionospheric delay. Both receivers compare the laboratory’s reference clock to GPST, and report the measurements in CGGTTS format files. In the measurements, the time scale of the timing laboratory was utilized as the reference clock for both receivers, allowing us to make a “common clock” measurement.

We computed the common-clock, common-view differences of measurements from the two receivers using no ionospheric delay correction, the MDIO, and the IGS MSIO corrections. We also computed the common-clock, common-view difference of the Rcvr (A) measurements with the P3 MSIO correction and the Rcvr (B) measurements with the IGS MSIO correction. Because the GPS time, the reference clock, and the ionospheric delay in the two measurements should completely cancel out in this type of

measurement, the difference should be zero for each of the ionospheric delay correction methods if the two receivers are calibrated. The non-zero time differences shown in Fig. 4 indicate that the two receivers are not calibrated with respect to each other. The differences with no ionospheric delay correction (shown in red), MDIO correction (shown in blue) and IGS MSIO correction (shown in black) are grouped together. Because these differences only involve the measurements on the L1 frequency, the non-zero difference comes from the error in the $INT DLY_{L1}$ correction of $REF - GPS$. There is an offset of about -1.5 ns between these differences and the difference when Rcvr (A)’s ionospheric delay correction was obtained from the P3 method (shown in green). This offset indicates an error in either RCVR(A)’s $INTDLY_{L1}$ or in RCVR(A) $INTDLY_{L2}$ or in both, that is, the delay of $(P1 - P2)$ is not in agreement with the delay of P1. Notice also there is a slope of about 0.5 ns in each of the differences over the 20 day period. This slope probably indicates that the delays of the two receivers are slowly changing with respect to each other, or it could possibly be caused by multipath changes.

The receiver delay variation due to daily or seasonal environment changes adds noise to the measurement, and delay changes due

to the aging or malfunction of components introduces time steps in the measurements. Figure 5 shows the daily averaged common-view differences between UTC(NIST) and a remote clock based on the P3 measurements. The distance between the remote clock location and NIST is more than 7 500 km. The P3 measurements at NIST were made by the NIST primary receiver and the P3 measurements in the remote clock location were made by two receivers, Rcvr (A) and Rcvr (C). The latitude of the remote clock location is about 39° north. The antennas for Rcvr (A) and Rcvr (C) are separated by about 4.7 m. All the three receivers are dual-frequency, multi-channel devices. The slope of the two differences in Fig. 5 comes from the frequency offset between UTC(NIST) and the remote clock.

From Fig. 5, we see the difference using Rcvr (A) included a time step on MJD 56377 (March 26, 2013). The change in the difference before and after the step (MJDs 56376 and 56378) is 3.399 ns. Because there is no time step in the difference using Rcvr (C) and no change in the Rcvr (A) settings, the time step was caused by the receiver delay change of Rcvr (A). Using the difference of Rcvr (C), we estimate the time change due to the frequency offset is 0.341 ns. The time step in the Rcvr (A) difference on MJD 56377 is 3.058 ns after correcting for the frequency offset.

To take a closer look at the Rcvr (A) receiver delay change, Fig. 6 shows the daily averaged common-view difference of UTC(NIST) – remote clock with pseudo-range measurements from the Rcvr (A) and the NIST receiver. The pseudo-range measurements from Rcvr (A) are corrected with the P3 MSIO (shown in blue) and the IGS MSIO (shown in red). The pseudo-range measurements from the NIST receiver are corrected with the P3 MSIO. We see the difference using the Rcvr (A) measurements with IGS MSIO corrections also took a time step on the same date (MJD 56377), but the time step is about 1.3 ns after the frequency offset correction. Because the pseudo-range measurements using the IGS MSIO corrections only involve the $INT DLY_{L1}$ in the $REF - GPS$ correction, we estimate the $INT DLY_{L1}$ changed by -1.3 ns. Using Eq. (2) with $\Delta(REF - GPS)_{P3} = 3$ ns and $\Delta INT DLY_{L1} = -1.3$ ns, the change of $INT DLY_{L2}$ is approximately -0.2 ns.

4. Summary

Ionospheric delays must be corrected to obtain the best results when utilizing GPS signals for time transfer applications. Without these corrections, the daytime pseudo-range measurements would contain errors as large as tens of nanoseconds. The pseudo-range measurements with the MDIO correction still contain a large amount of residual ionospheric delay error. For the measurement at NIST, the variation of the pseudo-range measurements with the MDIO correction is about 10 ns from daytime to nighttime. The MDIO correction also performs poorly during daytime solar flares or geomagnetic storms. For single frequency receivers, the use of the IGS MSIO correction greatly improves the ionospheric delay correction. The dual-frequency receivers can obtain ionospheric delay from the dual-frequency measurements. The ionosphere-free or P3 MSIO is the best method for ionospheric delay correction. However, the P3 MSIO correction requires the use of receiver delay. The receiver delay variation on either one frequency or both frequencies will introduce uncertainty in the ionospheric delay correction and therefore in the time transfer result. Using the P3 common-clock common-view to monitor the dual-frequency receiver delay change locally, we can identify receiver delay changes at the 1 ns level. Many recent successful GPS receiver calibrations reported 1 ns link calibration uncertainty [15]. To maintain time transfer accuracy at the nanosecond level, it is important to locally monitor receiver delay changes and to periodically calibrate the receiver delay.

This paper is a contribution of the U.S. Government and is not subject to copyright.

5. References

- [1] J. Klobuchar, "Ionospheric Time-Delay Algorithm for Single-Frequency GPS Users," *IEEE T. Aero. Elec. Sys.*, vol. AES-23, no. 3, pp. 325-331, 1987.
- [2] J. Klobuchar, "Ionospheric Corrections for Timing Applications," *Proceedings of the Precise Time and Time Interval Meeting (PTTI)*, pp. 193-203, 1988.
- [3] S. Schaer and W. Gurtner, "IONEX: The IONosphere Map EXchange Format Version 1," *Proceedings of the IGS AC Workshop*, Darmstadt, Germany, February 1998.
- [4] M. Alizadeh, H. Schuh, S. Todorova, and M. Schmidt, "Global Ionosphere Maps of VTEC from GNSS, Satellite Altimetry, and Formosat-3/COSMIC

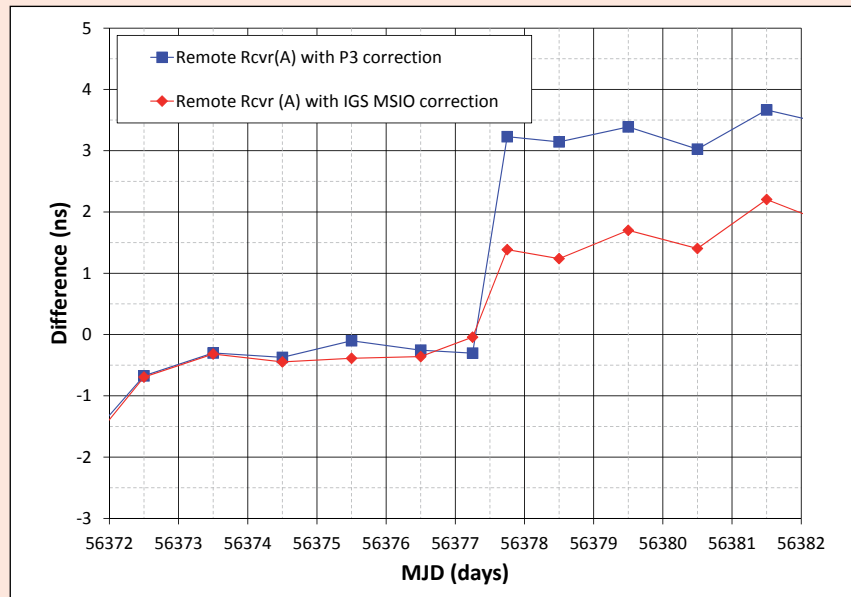


Figure 6. Daily averaged common-view differences of UTC(NIST) - remote clock. The pseudo-range measurements from Rcvr (A) are corrected with the P3 MSIO and the IGS MSIO. The pseudo-range measurements from the NIST receiver are corrected with P3 MSIO. Both differences show a time step of different sizes, indicating the Rcvr (A)'s receiver delays of L1 and L2 frequencies have both changed. The two points on MJD 56377 in each difference plot are the averaged differences before and after the time step.

Data," *J. Geodesy*, vol. 85, no. 12, pp. 975-987, 2011.

- [5] Information about the US regional ionosphere maps is available at: <http://www.ngdc.noaa.gov/stp/IONO/ionohome.html>
- [6] Information about the Europe regional ionosphere maps is available at: http://gnss.be/Atmospheric_Maps/ionospheric_maps.php
- [7] J. Ping, Y. Kono, K. Matsumoto, Y. Otsuka, A. Satito, C. Shum, K. Heki and N. Kawano, "Regional Ionosphere Map over Japanese Islands," *Earth Planets Space*, vol. 54, pp. e13-e16, 2002.
- [8] D. Allan and C. Thomas, "Technical Directives for Standardization of GPS Time Receiver Software," *Metrologia*, vol. 31, pp. 69-79, 1994.
- [9] J. Azoubib and W. Lewandowski, "CG-GTTS GPS/GLONASS Data Format Version 02," *7th CGGTTS meeting*, Reston, Virginia, November 1998.
- [10] D. Allan and M. Weiss "Accurate Time and Frequency Transfer during Common-view of a GPS Satellite," *Proceedings of the Frequency Control Symposium*, pp. 334-356, 1980.
- [11] Z. Jiang and G. Petit, "Time transfer with GPS satellites all in view," *Proceedings of the Asia-Pacific Workshop on Time and Frequency*, Beijing, China, pp. 236-243, October 2004.
- [12] M. Weiss, G. Petit, and Z. Jiang, "A Comparison of GPS Common-View Time Transfer to All-in-View," *Proceedings of the Joint 2005 IEEE Frequency Control Symposium and Precise Time and Time Interval (PTTI) Systems and Applications Meeting*, Vancouver, Canada, pp. 324-328, August 2005.
- [13] P. Defraigne and G. Petit, "Time Transfer to TAI Using Geodetic Receivers," *Metrologia*, vol. 40, pp. 184-188, 2003.
- [14] Information about the event can be found at (last accessed April 2015): <http://www.spaceweatherlive.com/community/topic/622-middle-latitude-auroral-activity-warning-february-27-28-2014/>
- [15] G. Rovera, J. Torre, R. Sherwood, M. Abgrall, C. Courde, M. Laas-Bourez, and P. Uhrich, "Link Calibration against Receiver Calibration: an Assessment of GPS Time Transfer Uncertainty," *Metrologia*, vol. 51, pp. 476-490, 2014.